JOURNAL OF EXPERIMENTAL AND THEORETICAL PHYSICS, 2024, Vol. 165, No. 2, pp. 265–282

STATISTICAL, NONLINEAR, AND SOFT MATTER PHYSICS

SCREENED AND VAN DER WAALS INTERACTIONS IN DUSTY PLASMA AND ELECTROLYTES

© 2024 A.V. Filippov

State Research Center of the Russian Federation Troitsk Institute for Innovation and Fusion Research, 108842 Troitsk, Moscow, Russia

Joint Institute for High Temperatures of the Russian Academy of Sciences Moscow, 125412 Russia

e-mail: fav@triniti.ru

Received September 01, 2023

Revised September 20, 2023

Accepted September 20, 2023

Abstract. Screened electrostatic and van der Waals interactions of nano- and micron-sized particles in dusty plasma were considered. The electrostatic interaction is considered on the basis of the linearized Poisson-Boltzmann equation for particles both with fixed charges uniformly distributed over their surfaces and with fixed surface electric potentials. The found solution of the problem makes it possible to study the interaction of both particles of comparable radius and particles of very different sizes. The interaction force takes into account the osmotic component, which in the case of constant charges leads to the restoration of the equality of the forces acting on the first and second particles. For the van der Waals interaction, the screening of static fluctuations and the retardation of electromagnetic fields for the dispersive part of the interaction were taken into account. Based on the analysis of various expressions for the geometric factor, taking into account the retardation of the electromagnetic field, a numerically stable method for calculating this factor was proposed. The total energy of interaction of two charged dust particles is calculated for plasma parameters characteristic of dusty plasma: the electron and ion number densities from 10^8 to 10^{12} cm^{-3}, the particle radius from 10 nm to 1 μm and the particle charges from 10 to 10^3 elementary charges per micron of particle radius.

Keywords: *screening*, *linearized Debye-Hückel equation*, *dusty plasma*, *dust particle*, *van der Waals interaction*, *geometric factor*, *retardation*

DOI: 10.31857/S00444510240213e1

1. INTRODUCTION

Interaction forces between charged surfaces, colloidal particles, ions and organic molecules dissolved in aqueous electrolyte play an important role in colloidal physics [1], biophysics [2], electro- and photo-catalysis [3], and environmental geochemistry [4]. These forces determine the stability of colloidal systems, dynamic properties and phenomena such as self-assembly in them [5-7], adsorption of ions on surfaces [8], adhesion of particles at the liquid-solid interface [9], and many other properties.

Studies of interaction forces at small distances are also important in the physics of dust plasma [10-22]. These forces play a particularly important role in the process of particle coagulation [23, 24]. Its study is also important for the development of a number of applications, such as the nanoparticle industry [25-29] and the formation of thin protective films or films with unique physical and chemical properties from them [30-33], in the accurate extraction of the van der Waals interaction at small distances [34-38], in the study of charged particle adhesion [39], modeling the process of removing small dust particles from the air using different types of gas discharge [40], etc.

To describe the interaction between micro- and nanoparticles, approximate approaches are currently mainly used (see, for example, the review [41]), in which the forces of electrostatic and van der Waals interaction are computed on the basis of the Deryagin approximation [42]. The electrostatic screened interaction is described by the Deryagin-Landau-Verwey-Overbeek theory (DLVO) [43]. In a number of works, the electrostatic interaction was considered more precisely on the

basis of the solution of the linearized Poisson-Boltzmann equation [44-53], while others developed very accurate methods for calculating the van der Waals interaction force (see, e.g., [54]). Below we present an exact solution of the problem of electrostatic interaction between nanoparticles based on the linearized Poisson-Boltzmann equation, which is supplemented with a description of the methodology for calculating the van der Waals interaction force. Based on the developed approaches, the total interaction energy of nano- and microparticles is calculated. The present work does not consider the interaction forces related to the finite size of electrolyte molecules, a modern description of which can be found in [55-57].

The present work is a continuation of [58, 59], in which special attention was paid to the case of constant particle surface potentials and their interaction in electrolytes at sufficiently high ion concentrations and, accordingly, high values of the screening constant. In the present work, the developed methods for calculating the interaction force taking into account plasma shielding will be tested by comparison with the solution of the interaction problem in vacuum [60-64]. Special attention will be paid to the interaction of particles in dust plasma.

2. SHIELDED ELECTROSTATIC INTERACTION

The geometry of the problem on the interaction of particles in the plasma taking into account the shielding effects is shown in Fig. 1. As in [46-49], we will consider the electrostatic interaction in the electrolyte in the framework of the linearized Poisson-Boltzmann model [65]:

$$\Delta\phi = k_D^2\phi, \tag{1}$$

where ϕ is the self-consistent electric field potential, k_D is the Debye shielding constant:

$$k_D^2 = \frac{4\pi e^2}{\varepsilon}\left(\frac{n_e}{T_e} + \frac{n_i z_i^2}{T_i}\right), \tag{2}$$

e - proton charge, ε - static dielectric permittivity of the medium, n_e - concentration of electrons or negative ions, n_i, z_i – concentration and charge number of positive ions, respectively, T_e, T_i – temperature of electrons or negative ions and positive ions in energy units.

The general solution of the Helmholtz equation (1) for the potential of the system of charges associated with the k-th particle in the spherical coordinate system with a pole in the center of this particle is defined by the expression (see, for example, [66]):

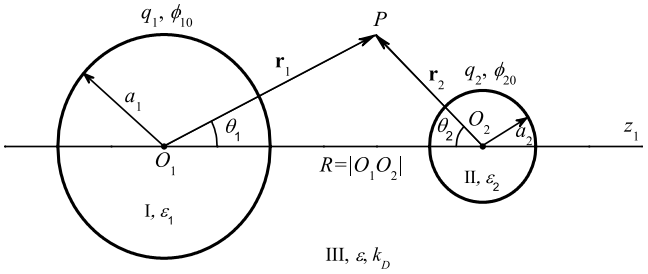

Fig. 1. Geometry of the problem on the interaction of particles in plasma taking into account shielding effects. Here q_i, ϕ_{i0}, a_i, ε_i – charge, surface potential, radius and dielectric constant of the i-th particle, respectively, $i = 1,2$, $\mathbf{r}_i$ – radius-vector of the observation point P, drawn from the center of the i-th particle O_i, θ_i – zenith angle in the spherical coordinate system with the pole in the center of the i-th particle and the axis, directed to the center of the other particle, R – interparticle distance, ε- dielectric permittivity of the electrolyte, k_D – inverse screening length (screening constant) of the plasma (electrolyte).

$$\phi_k = \sum_{n=0}^{\infty} A_{k,n} k_n\left(k_D r_k\right) P_n\left(\cos\theta_k\right), \tag{3}$$

where $A_{k,n}$ are the expansion coefficients, k_n are modified spherical Bessel functions of the 3rd kind:

$$k_n(x) = \sqrt{\frac{\pi}{2x}} K_{n+1/2}(x), \tag{4}$$

$K_{n+1/2}$ are modified Bessel functions of the 3rd kind (McDonald functions) [67]. To find the coefficients $A_{k,n}$ from the boundary conditions, we need to find the coefficients of the re-expansion of the potential of the *i-th* particle, written through Lejandre polynomials with a pole in the center of this particle, by Lejandre polynomials with a pole in the center of the other *k-th* macroparticle for which we will use the addition formula [44, 68]:

$$k_n\left(\tilde{r}_i\right) P_n\left(\cos\theta_i\right) = \\ = \sum_{m=0}^{\infty} \left(2m+1\right) L_{nm}\left(\tilde{R}\right) i_m\left(\tilde{r}_k\right) P_m\left(\cos\theta_k\right), \tag{5}$$

where $\tilde{r}_i = k_D r_i$, $\tilde{r}_k = k_D r_k$, $\tilde{R} = k_D R$, R is the distance between the centers of macroparticles, $i = 1,2$, $k = 3 - i$, $i_n(x)$ – modified spherical Bessel functions of the 1st kind:

$$i_n(x) = \sqrt{\frac{\pi}{2x}} I_{n+1/2}(x), \tag{6}$$

I_{n+12} – modified Bessel functions of the 1st kind (Infeld functions) [67], R-dependent coefficients of L_{mn} are defined by the sum of

$$L_{nm}\left(\widetilde{R}\right) = \sum_{\ell=0}^{\min\{n,m\}} k_{n+m-2\ell}\left(\widetilde{R}\right) G_{nm}^{\ell}, \tag{7}$$

$$G_{nm}^{\ell} = \frac{(n+m-\ell)!\left(n+m-2\ell+1/2\right)}{\ell!(n-\ell)!(m-\ell)!} \times \\ \times \frac{1}{\pi} \frac{\Gamma\left(n-\ell+1/2\right)\Gamma\left(m-\ell+1/2\right)\Gamma\left(\ell+1/2\right)}{\Gamma\left(m+n-\ell+3/2\right)}, \tag{8}$$

where $\Gamma(x)$ is the the gamma function:

$$\Gamma\left(n+1/2\right) = \sqrt{\pi}\frac{\left(2n-1\right)!!}{2^n}, \tag{9}$$

$\left(2n-1\right)!! = 1\cdot 3\cdot \ldots \cdot (2n-1)$. In expression (7) and below, the values reduced to the Debye radius are marked with a tilde: $\widetilde{R} = k_D R$. Note that $G_{nm}^{\ell} = G_{mn}^{\ell}$ and hence $L_{nm} = L_{mn}$ (Regarding the calculation of the coefficients of G_{nm}^{ℓ} see. Appendix A.)

Finally, for the potential of the *i-th* particle we obtain an expression through Lejandre polynomials with a pole at the center of the *k-th* macroparticle (i = 1, 2, k = 3 - i):

$$\phi_i\left(\tilde{r}_k, \theta_k\right) = \\ = \sum_{n=0}^{\infty}\sum_{m=0}^{\infty} A_{i,m} b_{nm}\left(\tilde{r}_k, \widetilde{R}\right) P_n\left(\cos\theta_k\right), \tag{10}$$

where the coefficients b_{nm} are determined by the expression:

$$b_{nm}\left(\tilde{r}_k, \widetilde{R}\right) = \left(2n+1\right) i_n\left(\tilde{r}_k\right) L_{mn}\left(\widetilde{R}\right). \tag{11}$$

In [46-49], the coefficients b_{nm} were defined as double sums from products of modified Bessel functions of the 1st and 3rd kinds, and expression (11) contains only a single summation when calculating L_{mn}. Numerical calculations have shown that the coefficients b_{nm}, calculated by (11) and the formulas given in [46-49], coincide within the limits of calculation errors with double precision on the computer.

In plasma or electrolyte, depending on the parameters of the plasma and particles of the condensed disperse phase, either the regime of constancy of the macroparticle surface potentials or the regime of constancy of their charges can be realized (for a detailed discussion of this issue for electrolytes, see [49]). For macroparticles with radius of 1 μm and more and at sufficiently high plasma concentration $n_i > 10^9 \text{cm}^{-3}$, when the interparticle distance changes with the thermal velocity of macroparticles, their surface potential $\phi_{i,0}$, which coincides with the floating plasma potential, is constant. For nanoparticles with a radius of about 100 nm or less and at sufficiently low plasma concentration $n_i < 10^9 \text{cm}^{-3}$, the constant charge regime is realized. Therefore, in the present work we consider both modes of convergence of nano- or macroparticles.

2.1. Constant charge mode

Boundary conditions at the particle surface in this case are [69, 70]

$$\phi_{\text{I}}\big|_{r_1=a_1} = \left(\phi_1+\phi_2\right)\big|_{r_1=a_1}, \\ \phi_{\text{II}}\big|_{r_2=a_2} = \left(\phi_1+\phi_2\right)\big|_{r_2=a_2}, \tag{12}$$

$$\varepsilon_1 \frac{\partial\phi_{\text{I}}}{\partial r_1}\bigg|_{r_1=a_1-0} - \varepsilon \frac{\partial\left(\phi_1+\phi_2\right)}{\partial r_1}\bigg|_{r_1=a_1+0} = 4\pi\sigma_1, \\ \varepsilon_2 \frac{\partial\phi_{\text{II}}}{\partial r_2}\bigg|_{r_2=a_2-0} - \varepsilon \frac{\partial\left(\phi_1+\phi_2\right)}{\partial r_2}\bigg|_{r_2=a_2+0} = 4\pi\sigma_2, \tag{13}$$

where ϕ_{I}, ϕ_{II} are the electric field potentials inside the 1st and 2nd particles, respectively, ε_1, ε_2 are their dielectric permittivities, σ_1 and σ_2 are the charge density distributions on their surfaces.

The general solution of the Laplace equation inside a homogeneous dielectric, taking into account the requirement of finiteness of the potential inside nanoparticles, can be written as [69, 70]

$$\phi_{\text{I}}\left(r_1,\theta_1\right) = \sum_{n=0}^{\infty} C_n P_n\left(\cos\theta_1\right)\tilde{r}_1^n, \\ \phi_{\text{II}}\left(r_2,\theta_2\right) = \sum_{n=0}^{\infty} D_n P_n\left(\cos\theta_2\right)\tilde{r}_2^n, \tag{14}$$

where C_n, D_n are the expansion coefficients.

Using expressions (10) and (14), from the boundary conditions (12) and (13) for the potential expansion coefficients ϕ_1 and ϕ_2 we obtain a system of equations (n = 0,1,...)

$$\alpha_{1,n} A_{1,n} + \sum_{m=0}^{\infty} \beta_{1,nm} A_{2,m} = \frac{4\pi}{k_D}\sigma_{1,n}, \\ \alpha_{2,n} A_{2,n} + \sum_{m=0}^{\infty} \beta_{2,nm} A_{1,m} = \frac{4\pi}{k_D}\sigma_{2,n}, \tag{15}$$

where coefficients $\alpha_{i,n}$ and $\beta_{i,nm}$, $i = 1,2$, are defined by the relations

$$\alpha_{i,n} = \varepsilon k_{n+1}(\tilde{a}_i) + \frac{n(\varepsilon_i - \varepsilon)}{\tilde{a}_i} k_n(\tilde{a}_i),$$
$$\beta_{i,nm} = \frac{n\varepsilon_i}{\tilde{a}_i} b_{nm}(\tilde{a}_i, \tilde{R}) - \varepsilon \frac{\partial b_{nm}(\tilde{a}_i, \tilde{R})}{\partial \tilde{a}_i}, \quad (16)$$

$\sigma_{i,n}$ – expansion coefficients of the surface charge density by Lejandre polynomials:

$$\sigma_{i,n} = \frac{2n+1}{2} \int_{-1}^{1} P_n(\mu_i)\sigma_i(\mu_i)d\mu_i. \quad (17)$$

It is taken into account here that in this paper we consider the surface charge distribution axially symmetric about the z-axis. In the case of uniform distribution of free charges only the term with $n = 0$ will be different from zero:

$$\sigma_{i,0} = \frac{q_i}{4\pi a_i^2}, i = 1,2. \quad (18)$$

Let us rewrite the system (15) by excluding the coefficients $A_{2,m}$ from the first equation using the second equation. As a result, we obtain

$$A_{1,n} - \sum_{k=0}^{\infty} A_{1,k} \sum_{m=0}^{\infty} \frac{\beta_{1,nm}\beta_{2,mk}}{\alpha_{1,n}\alpha_{2,m}} = \frac{\sigma_{1,n}}{\alpha_{1,n}} - \sum_{m=0}^{\infty} \frac{\beta_{1,nm}}{\alpha_{1,n}\alpha_{2,m}} \sigma_{2,m}, \quad n = 0,1,\ldots \quad (19)$$

The system of equations (19) allows us to determine the expansion coefficients of the potential of the first particle and, using the second equation of the system (15), to determine the expansion coefficients of the potential of the second particle.

From (7), (11) and (16) we see that the values $\beta_{i,nm}$ are the sum, each term of which contains a spherical Macdonald function, namely $k_{n+m-2\ell}(\tilde{R})$, $\ell = 0,1,\ldots,\max\{n,m\}$, therefore they have a common denominator $\exp(-\tilde{R})$. Hence, the product $\beta_{1,nm}\beta_{2,mk}$ includes a common $\exp(-2\tilde{R})$ denominator. Now, neglecting the terms containing $\exp(-2\tilde{R})$ and higher degrees, from (19) and the analogous equation for the 2nd particle in the case of uniform charging of the particles we can find

$$A_{i,n} \approx \frac{4\pi}{k_D \alpha_{i,n}} \sigma_{i,n}\delta_{n,0} - \frac{4\pi}{k_D} \frac{\beta_{i,n0}}{\alpha_{i,n}\alpha_{3-i,0}} \sigma_{3-i,0}. \quad (20)$$

From (11) at $m = 0$ we have

$$b_{n0}(\tilde{r}_k, \tilde{R}) = (2n+1) i_n(\tilde{r}_k) k_n(\tilde{R}). \quad (21)$$

Now, using the definitions (16), we obtain (see [71])

$$A_{i,n} \approx \frac{4\pi\sigma_{i,0}}{\varepsilon k_D k_1(\tilde{a}_i)}\delta_{n,0} - \frac{4\pi\sigma_{3-i,0}}{\varepsilon k_D k_1(\tilde{a}_{3-i})}(2n+1) k_n(\tilde{R}) M_n(\tilde{a}_i, \varepsilon, \varepsilon_i), \quad (22)$$

where M_n are functions defined by the relation (see [71])

$$M_n(\tilde{a}_i, \varepsilon, \varepsilon_i) = \frac{n(\varepsilon_i - \varepsilon) i_n(\tilde{a}_i) - \varepsilon \tilde{a}_i i_{n+1}(\tilde{a}_i)}{\varepsilon \tilde{a}_i k_{n+1}(\tilde{a}_i) + n(\varepsilon_i - \varepsilon) k_n(\tilde{a}_i)}. \quad (23)$$

At $a_2 = 0$ this solution passes to the solution of the problem of interaction of a point charge with a dielectric ball in a plasma (see [71]). As the number n increases, the value of the functions i_n grows and k_n falls, and the value of the product $i_n(x)k_n(x)$ decreases very slowly. The rate of decrease can be judged by the relation [67]

$$k_n(x) i_{n+1}(x) + k_{n+1}(x) i_n(x) = \frac{\pi}{2x^2}. \quad (24)$$

Therefore, the calculation of the coefficients $A_{i,n}$ with acceptable accuracy requires taking into account a large number of terms. Below the approximate solution (22) will be used to determine the number of considered terms of the potential decomposition.

2.2. Constant Surface Potential Mode

In the case when the characteristic time of charging of particles considerably exceeds the characteristic time of changing the distance between them, the regime of constant surface potentials is realized, which are determined by the floating potential of the plasma. Note that in the case of conducting particles the surface potential is also constant in the in the sense that it does not depend on angular variables, but at a constant charge it changes at changing of the interparticle distance. In the regime of constant, not depending on the interparticle distance of the particle surface potentials $\phi_{i,0}$, $i = 1,2$, the solution of the problem considered here is considerably simplified and to find the expansion coefficients from the condition of continuity of the potential at the interface of dielectric media [69] we obtain a system of equations ($n = 0,1,\ldots,$):

$$k_n(\tilde{a}_1)A_{1,n} + \sum_{m=0}^{\infty} b_{nm}(\tilde{a}_1, \tilde{R})A_{2,m} = \phi_{1,0}\delta_{n0},$$
$$k_n(\tilde{a}_2)A_{2,n} + \sum_{m=0}^{\infty} b_{nm}(\tilde{a}_2, \tilde{R})A_{1,m} = \phi_{2,0}\delta_{n0}. \quad (25)$$

Having excluded $A_{2,n}$ from the first equation with the help of the second, after changing the order of summation we obtain

$$A_{1,n} - \sum_{k=0}^{\infty} A_{1,k} \sum_{m=0}^{\infty} \frac{b_{nm}(\tilde{a}_1, \tilde{R})b_{mk}(\tilde{a}_2, \tilde{R})}{k_n(\tilde{a}_1)k_m(\tilde{a}_2)} =$$
$$= \phi_{1,0}\frac{\delta_{n0}}{k_n(\tilde{a}_1)} - \phi_{20}\frac{(2n+1)i_n(\tilde{a}_1)k_n(\tilde{R})}{k_0(\tilde{a}_2)k_n(\tilde{a}_1)}. \quad (26)$$

If we neglect the terms containing $\exp(-2\tilde{R})$ and higher degrees, we find from (26)

$$A_{i,n} \approx \frac{\phi_{i,0}}{k_0(\tilde{a}_i)}\delta_{n0} - (2n+1)\frac{i_n(\tilde{a}_i)k_n(\tilde{R})}{k_n(\tilde{a}_i)k_0(\tilde{a}_{3-i})}\phi_{3-i,0}. \quad (27)$$

The charges of particles in the regime of constant potentials become functions of the interparticle distance. From the boundary condition of continuity of electric induction (13) for determination of charges we obtain the expressions

$$q_i = \varepsilon a_i \tilde{a}_i \left[k_1(\tilde{a}_i)A_{i,0} - i_1(\tilde{a}_i)\sum_{m=0}^{\infty} k_m(\tilde{R})A_{3-i,m} \right], \quad i = 1,2. \quad (28)$$

After simple transformations using (25) and relation (24), from (28) we can get the following:

$$q_i = \frac{\varepsilon a_i}{\sinh(\tilde{a}_i)}\left\{ \frac{\pi}{2}A_{i,0} - \left[\tilde{a}_i\cosh(\tilde{a}_i) - \sinh(\tilde{a}_i)\right]\phi_{i,0} \right\}. \quad (29)$$

From (28), another expression for determining the charge can be obtained:

$$q_i = q_{i,\infty} - \varepsilon a_i e^{\tilde{a}_i} \sum_{m=0}^{\infty} k_m(\tilde{R})A_{3-i,m}, \quad (30)$$

which explicitly contains the relation of the charge to the potential of a solitary particle:

$$q_{i,\infty} = \varepsilon a_i \phi_{i,0}(1 + \tilde{a}_i), \quad (31)$$

since for the particles removed from each other on a large distance, $R \to \infty$, their influence on each other is negligibly small. In this case it follows from (27)

$$A_{i,0}^{\infty} = \frac{\phi_{i0}}{k_0(\tilde{a}_i)} = \frac{2}{\pi}\phi_{i0}\tilde{a}_i e^{\tilde{a}_i}, i = 1,2. \quad (32)$$

The relation (31) can also be obtained from a comparison of expressions (27) and (32), which must coincide when $R \to \infty$

2.3. Determining the interaction force

In [46, 47], to find the force, we use the Maxwell tension tensor:

$$T_{\mathbf{n},i} = \frac{\varepsilon}{4\pi}\left(E_n\mathbf{E} - \frac{1}{2}\mathbf{n}E^2 \right)\Big|_{r=a_i}, \quad (33)$$

where $\mathbf{E} = -\nabla\phi$, $\mathbf{n}$ is the vector of the external normal to the surface of the i-th particle, $E_n = \mathbf{E}\cdot\mathbf{n}$. As a result of integration by angles for the z-component of the force acting on the i-th particle, the following expression was obtained

$$F_{i,z} = \varepsilon\sum_{n=1}^{\infty}\frac{n}{(2n-1)(2n+1)}\left[\begin{matrix}\Xi_{i,n-1} - \\ -(n-1)\Psi_{i,n-1}\end{matrix}\right]\times \left[\Xi_{i,n} + (n+1)\Psi_{i,n}\right], \quad (34)$$

where

$$\Xi_{i,n} = A_{i,n}\left[nk_n(\tilde{a}_i) - \tilde{a}_i k_{n+1}(\tilde{a}_i) \right] + \sum_{m=0}^{\infty} A_{3-i,m}\tilde{a}_i\frac{\partial b_{nm}(\tilde{a}_i, \tilde{R})}{\partial\tilde{a}_i}, \quad (35)$$

$$\Psi_{i,n} = A_{i,n}k_n(\tilde{a}_i) + \sum_{m=0}^{\infty} A_{3-i,m}b_{nm}(\tilde{a}_i, \tilde{R}). \quad (36)$$

Note that according to Fig. 1, the z-axis for the second particle is directed to the left.

In [72, 73], an expression was proposed to determine the density of surface forces associated with osmotic pressure at the surface particles, which in [74] was transformed into the usual Maxwell tension tensor:

$$T_{i,\alpha\beta}^{o} = -\frac{\varepsilon}{4\pi}k_D^2\phi^2\Big|_{r=a_i}\delta_{\alpha\beta}, \quad (37)$$

where $\alpha,\beta = x,y,z$. For the problem considered in this paper, only the z-component of the Maxwell tension tensor is significant:

$$T^o_{i,rz} = -\frac{\varepsilon}{4\pi}k_D^2\phi^2\Big|_{r=a_i}\cos\theta. \tag{38}$$

Thus, for the osmotic component of the force we find

$$F^o_{i,z} = \int\limits_S T_{i,rz}dS_i = -\frac{\varepsilon}{2}a_i^2k_D^2\int\limits_0^\pi\phi^2\Big|_{r=a_i}\cos\theta\sin\theta d\theta = \\ = -\varepsilon\tilde{a}_i^2\sum_{n=1}^{\infty}\frac{n\Psi_{i,n-1}\Psi_{i,n}}{(2n-1)(2n+1)}, \tag{39}$$

where the value of $\Psi_{i,n}$ is defined by expression (36).

2.3.1. Constant charges of particles

In the case of constant charges of particles, the osmotic component of the force is different from zero, so adding $F_{i,z}$and $F^o_{i,z}$, for the total interaction force from (34) and (39) we obtain

$$F^t_{i,z} = \varepsilon\sum_{n=1}^{\infty}\frac{n}{(2n-1)(2n+1)}\times \\ \times\left\{\begin{array}{c}\left[\Xi_{i,n-1}-(n-1)\Psi_{i,n-1}\right]\times\\ \times\left[\Xi_{i,n}+(n+1)\Psi_{i,n}\right]-\\ -\tilde{a}_1^2\Psi_{i,n-1}\Psi_{i,n}\end{array}\right\}. \tag{40}$$

Let's exclude the derivative $\partial b_{nm}/\partial\tilde{a}_i$ in the expression (35) for $\Xi_{i,n}$ with the equations (15) and after simple transformations we find

$$\Xi_{i,n} = -\frac{4\pi a_i}{\varepsilon}\sigma_{i,n} + \frac{n\varepsilon_i}{\varepsilon}\Psi_{i,n}. \tag{41}$$

As a result, from (40) we obtain

$$F^t_{1,z} = -\frac{q_1}{a_1}\frac{\varepsilon_1+2\varepsilon}{3\varepsilon}\Psi_1 + \\ +\sum_{n=1}^{\infty}\frac{(n-1)(\varepsilon_1-\varepsilon)\left[n\varepsilon_1+\varepsilon(n+1)\right]-\varepsilon^2\tilde{a}_1^2}{\varepsilon(2n-1)(2n+1)}\times \\ \times n\Psi_{n-1}\Psi_n. \tag{42}$$

Then we obtain the expression for the interaction force at $k_DR \gg 1$, neglecting the terms containing the $\exp(-2\tilde{R})$ and higher degrees. Using (20) or (22), we find from (34)

$$F_{1,z} = -\frac{q_1q_2}{\varepsilon R^2}\frac{1+\tilde{R}}{(1+\tilde{a}_1)(1+\tilde{a}_2)}e^{-k_DL}\times \\ \times\left(1+\frac{\varepsilon}{\varepsilon_1+2\varepsilon}\frac{\tilde{a}_1^2}{1+\tilde{a}_1}\right)^{-1}. \tag{43}$$

This expression shows the inequality of forces: $F_{1,z} \neq F_{2,z}$, which was emphasized in [46, 47]. Thus, for the osmotic component of the force (39) with the same accuracy we find

$$F^o_{1,z} = -\frac{q_1q_2}{R^2}e^{-k_DL}\frac{(1+\tilde{R})}{(1+\tilde{a}_1)(1+\tilde{a}_2)}\times \\ \times\frac{\tilde{a}_1^2}{(\varepsilon_1+2\varepsilon)(1+\tilde{a}_1)+\varepsilon\tilde{a}_1^2}. \tag{44}$$

Summarizing (43) and (44), for the total force we find symmetric with respect to the permutation of particles, well known expression in the Deryagin approximation [43]:

$$F^D_z = -\frac{q_1q_2}{\varepsilon R^2}\frac{1+\tilde{R}}{(1+\tilde{a}_1)(1+\tilde{a}_2)}e^{-k_DL}. \tag{45}$$

This expression can also be obtained directly from (42).

2.3.2. Constant surface potentials particles

In the case of constant particle surface potentials, using expression (25), from (36) we find

$$\Psi_{i,0} = \phi_{i,0}, \Psi_{i,n} = 0, n \geq 1. \tag{46}$$

In this case, the osmotic component of the force disappears and to determine the force in the case of constant particle surface potentials from expression (34) as follows

$$F_{i,z} = \varepsilon\sum_{n=1}^{\infty}\frac{n\Xi_{i,n-1}\Xi_{i,n}}{(2n-1)(2n+1)}. \tag{47}$$

For the value Ξ_n, using the properties of modified spherical Bessel functions [67] and the first equation of the system (25), we can obtain

$$\Xi_n = \tilde{a}_1 \frac{i_{n+1}(\tilde{a}_1)}{i_n(\tilde{a}_1)}\phi_{10}\delta_{n0} - \frac{\pi}{2\tilde{a}_1 i_n(\tilde{a}_1)}A_{1,n}. \quad (48)$$

As a result, the expression for the force (47) takes the form

$$F_{i,z} = -\varepsilon\frac{\pi}{6}\frac{A_{1,1}}{i_0(\tilde{a}_1)}\phi_{1,0} + \varepsilon\left(\frac{\pi}{2\tilde{a}_1}\right)^2 \times \times \sum_{n=1}^{\infty}\frac{n}{(2n-1)(2n+1)}\frac{A_{1,n-1}A_{1,n}}{i_{n-1}(\tilde{a}_1)i_n(\tilde{a}_1)}. \quad (49)$$

At large distances, if the condition $k_D R \gg 1$ is satisfied, neglecting the terms containing $\exp(-2\tilde{R})$ and higher degrees, using (27), we find from (49) the well-known expression for the force in the Deryagin approximation [43]:

$$F_{\text{DLVO}} = -\varepsilon\phi_{1,0}\phi_{2,0}\frac{\pi}{2}\frac{k_1(\tilde{R})}{k_0(\tilde{a}_1)k_0(\tilde{a}_2)} \equiv \equiv -\varepsilon\phi_{1,0}\phi_{2,0}\frac{a_1 a_2}{R^2}(1+k_D R)e^{-k_D L}, \quad (50)$$

where $L = R - a_1 - a_2$.

Fig. 2 compares the interaction force between two particles of the same (*a*) and different radii (*b*) at different plasma densities from $n_e = n_i = 10^8$ to 10^{12} cm^{-3} with the interaction force in vacuum ($\varepsilon = 1$). It can be seen that at low plasma density at small distances the shielding effects are negligibly small and the electrostatic interaction force in plasma is practically no different from the electrostatic interaction force in vacuum. As the plasma density increases, the shielding effect increases and appears already at small distances between the surfaces of particles.

2.4. Particle electrostatic interaction potential

After integrating (50) and (45), we obtain the well-known expressions for the electrostatic potential in the Deryagin approximation [43]:

$$U_D = \varepsilon\phi_{1,0}\phi_{2,0}\frac{a_1 a_2}{R}e^{-\tilde{L}} = = \frac{q_1 q_2}{\varepsilon R}\frac{e^{-k_D L}}{(1+\tilde{a}_1)(1+\tilde{a}_2)}. \quad (51)$$

The transition from this formula to another one is easily accomplished by using the relation (31).

In [72], an expression for the free energy or interaction potential of particles was proposed on the basis of thermodynamic considerations:

$$U(R) + U_\infty = = \int\limits_{S_1+S_2}\left[Q_s(\phi_s, r_s) - \frac{1}{2}\phi_s\sigma_s(\phi_s, r_s)\right]dS, \quad (52)$$

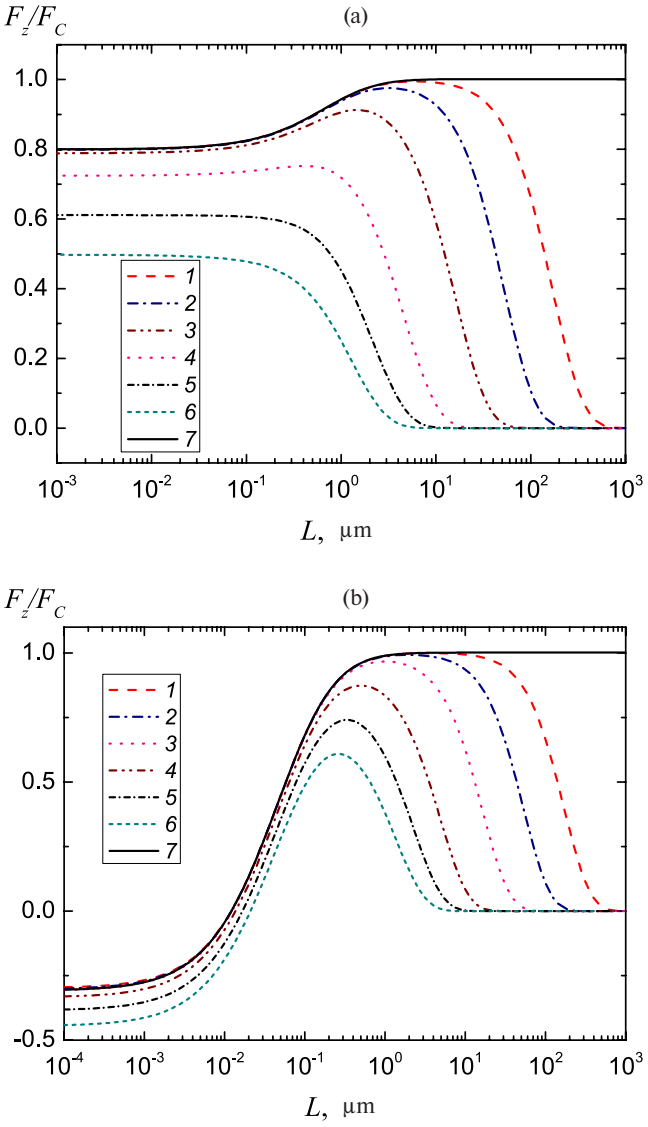

Fig. 2. Dependences of the reduced to Coulomb $F_C = q_1 q_2/R^2$ interaction force F_z of two particles at $T_e = T_i = 300$ K, $a_1 = a_2 = 1$ μm, $q_1 = q_2 = 100e$ (*a*) and $a_1 = 1$ μm, $a_2 = 100$ nm, $q_1 = 100e$, $q_2 = 10e$ (*b*) at different concentrations of electrons and ions in the plasma (the Debye radius $R_D = 1/k_D$ in μm is given in brackets): *1* — $n_e = 10^8$ (84.6), *2* — 10^9 (26.7), *3* — 10^{10} (8.46), *4* — 10^{11} (2.67), *5* — $4{\cdot}10^{11}$ (1.34), *6* — 10^{12} cm^{-3} (0.85), *7* — in vacuum.

where ϕ_s is the particle surface potential, generally depending on the angular variables of the spherical coordinate system with a pole at the center of the particle: $\phi_s = \phi_s(\theta,\varphi)$, r_s is the radial coordinate of the particle surface, σ_s is the surface charge density: $\sigma_s = \sigma_s(\theta,\varphi)$, U_∞ provides zeroing of the interaction potential at R_∞, Q_s is a functional integral:

$$Q_s(\phi_s, r_s) = \int_{\phi_s} d\phi_s' \sigma_s(\phi_s', r_s). \quad (53)$$

The integration in (52) is over the surface of the first S_1 and second S_2 particles.

2.4.1. Constant charges of particles

In the case of uniform and fixed free surface charge density, integration (53) gives $Q_s = \phi_s\sigma_s$ and from (52):

$$U(R) = \frac{1}{2}\left[2\pi a_1^2\sigma_1\int_{-1}^{1}(\phi_1+\phi_2)\Big|_{r=a_1} d\mu_1 + \right.$$
$$\left. + 2\pi a_2^2\sigma_2\int_{-1}^{1}(\phi_1+\phi_2)\Big|_{r_2=a_2} d\mu_2\right] - U_\infty. \quad (54)$$

Hence, using expressions (3) and (10) expressed in the coordinate system corresponding to each particle, we obtain:

$$U_\sigma(R) = \frac{1}{2}\left[q_1(\phi_{1,s} - \phi_{1,\infty}) + q_2(\phi_{2.s} - \phi_{2,\infty})\right], \quad (55)$$

where $\phi_{i,s}$ is the angularly averaged surface potential of the i-th particle:

$$\phi_{i,s}(R) = k_0(\tilde{a}_i)A_{i,0} + \sum_{m=0}^{\infty} b_{0m}(\tilde{a}_i, \tilde{R})A_{3-i,m}, \quad (56)$$

$\phi_{i,\infty}$ is the particle surface potential at infinite distance from each other, which is determined by an expression similar to relation (31):

$$\phi_{i,\infty} = \frac{q_i}{\varepsilon a_i}\frac{1}{(1+\tilde{a}_i)}. \quad (57)$$

Note that the calculation of the interaction potential from (55) is considerably simplified by using the relation

$$\phi_{i,s}(R) - \phi_{i,\infty} = \frac{A_{i,0} - A_{i,0}^{\infty}}{i_1(\tilde{a}_i)}\frac{\pi}{2\tilde{a}_i^2},$$

$$A_{i,0}^{\infty} = \frac{2}{\pi}\frac{q_i}{k_D\varepsilon(1+\tilde{a}_i)}e_i^{\tilde{a}}. \quad (58)$$

At large distances, the difference (58) comes out to the asymptotics of the DLVO potential

$$\phi_{1,s}^{D}(R) - \phi_{1,\infty} = \frac{q_2}{\varepsilon(1+\tilde{a}_1)(1+\tilde{a}_2)R}e^{-\tilde{R}+\tilde{a}_1+\tilde{a}_2}.$$

2.4.2. Constant potentials of the particle surface

In the case of constant surface potentials, it follows from (53) that $Q_s = 0$ and in this case, we have the expression for the determination of the interaction potential:

$$U_\phi(R) - U_\infty = -\frac{1}{2}\left[\int_{S_1}\phi_{1,0}\sigma_1 dS_1 + \int_{S_2}\phi_{2,0}\sigma_2 dS_2\right]. \quad (59)$$

Integration (59) leads to the following expression for determining the electrostatic interaction potential in the case of constant particle surface potentials:

$$U_\phi(R) = -\frac{1}{2}\left\{\begin{array}{l}\phi_{1,0}\left[q_1(R) - q_{1\infty}\right] \\ +\phi_{2,0}\left[q_2(R) - q_{2\infty}\right]\end{array}\right\}, \quad (60)$$

where $q_{1,\infty}$, $q_{2,\infty}$ are the charges of particles at $R = \infty$ [see expression (31)].

Numerical calculations have shown that the values of the electrostatic interaction potential determined from expressions (58) or (60) and found by integrating the dependence of the interaction force on the distance between particles differ no more than the accuracy of the solution of equations (15) or (25) by the LU-decomposition method [75].

3. VAN DER WAALS INTERACTION

The theory of interaction of solids due to fluctuations of the electric field began to develop with the work [76], in which an expression for the interaction potential of solids was obtained by summing the van der Waals pairwise interaction of all atoms composing the bodies. In [77], the interaction potentials of an atom with a perfectly conducting wall and with another atom were found, taking into account the retardation of the electromagnetic field. In [78] a more accurate theory of the interaction between two infinite planar dielectrics separated by vacuum was constructed, and

in [79] – separated by liquid. The general theory of the van der Waals interaction is stated in many papers (see, for example, [80-82]).

Today, due to the complexity of the theory in the general case, to determine the Hamaker constant for the interaction 1st dielectric – liquid (vacuum) – 2nd dielectric we can use expression:

$$A_{132} = \frac{3\hbar}{4\pi}\int_0^\infty \frac{(\varepsilon_1 - \varepsilon_3)(\varepsilon_2 - \varepsilon_3)}{(\varepsilon_1 + \varepsilon_3)(\varepsilon_2 + \varepsilon_3)} d\xi, \tag{61}$$

obtained in [79] and valid at negligibly small distances between dielectrics. Here ε_1, ε_2, ε_3 are dielectric permittivities of bodies and liquid (gas) medium, frequency dependences of which are taken at imaginary frequency $i\xi$.

The potential of van der Waals interaction in a dielectric fluid of two dielectric particles of spherical shape without taking into account the retardation effects by a method close to the one used in [78] was obtained in [83] for the case $L \ll a_1, a_2$

$$U_{vdW} = -\frac{2\pi a_1 a_2 L}{(a_1 + a_2)} \frac{A_{131}}{12\pi L^2}, \tag{62}$$

where A_{131} is the Hamaker constant defined by relation (61). In [83], the following approximation term is also obtained, which requires the calculation of the analog of the Hamaker constant by a different from (61) formula.

In the present paper, the vdW interaction potential is determined according to [54] by expression

$$U_{vdW} = -\frac{1}{12}\left(A_0 f_{sh} F_H + A_1 F_g\right), \tag{63}$$

where A_0 is the contribution of zero oscillations to the Hamaker constant, which is shielded but does not experience retardation effects, A_1 is the dispersive contribution to the Hamaker constant, which is retarded but not shielded, f_{sh} is the shielding factor, F_H is the geometric Hamaker factor, F_g is the geometric factor taking into account the retardation of the fluctuating electromagnetic field. The contribution of zero fluctuations (constant A_0) and the dispersion contribution (constant A_1) to the Hamaker constant were calculated according to [54, 84]:

$$A_0 = \frac{3}{4} k_B T \left[\frac{\varepsilon_1(0) - \varepsilon_2(0)}{\varepsilon_1(0) + \varepsilon_2(0)}\right]^2, \tag{64}$$

$$A_1 = \frac{3\hbar}{64}\frac{\sqrt{\omega_1\omega_2}}{n_m^{7/2}} \times \times \frac{X^2 n_m^2 + 2X\Delta\varepsilon_0 n_m + \Delta\varepsilon_0^2(3 + 2Y)}{\left(\sqrt{Y - \sqrt{Y^2 - 1}} + \sqrt{Y + \sqrt{Y^2 - 1}}\right)^3}, \tag{65}$$

where $\hbar$ is Planck's constant, $\varepsilon_1(0)$ and $\varepsilon_2(0)$ are static dielectric permittivities of media 1 and 2, n_{01} and n_{02} are refractive indices, ω_1 and ω_2 are absorption frequencies, the values n_m, $\Delta\varepsilon_0$, X and Y are determined by the relations

$$n_m^2 = \frac{1}{2}\left(n_{01}^2 + n_{02}^2\right), \quad \Delta\varepsilon_0 = n_{01}^2 - n_{02}^2, \tag{66}$$

$$X = \frac{\omega_1}{\omega_2}\left(n_{01}^2 - 1\right) - \frac{\omega_2}{\omega_1}\left(n_{02}^2 - 1\right),$$
$$Y = \frac{1}{4\sqrt{n_m}}\left[\frac{\omega_1}{\omega_2}\left(n_{01}^2 + 1\right) + \frac{\omega_2}{\omega_1}\left(n_{02}^2 + 1\right)\right]. \tag{67}$$

The shielding factor in (63) was determined by the expression [54]

$$f_{sc} = (1 + 2k_D L)\exp(-2k_D L). \tag{68}$$

The geometric Hamaker factor in expression (63) was calculated according to the expression [76]

$$F_H = \left[4a_1 a_2\left(\frac{1}{D_1} + \frac{1}{D_2}\right) + 2\ln\frac{D_1}{D_2}\right]. \tag{69}$$

A number of works are devoted to the calculation of the geometric factor taking into account the retardation, among which we will focus on the following ones. All of them are based on one or another approximation of the contribution of retardation effects to the interaction potential of atoms, based on [77]. In [85] there were proposed the following approximation:

$$0 < p \le 3, \quad f(p) = 1.01 - 0.14p,$$
$$p \ge 3, \quad f(p) = \frac{2.45}{p} - \frac{2.04}{p^2}, \tag{70}$$

where $p = 2\pi r / \lambda_0$, r is the distance between atoms. On the basis of this approximation, the following formulas for calculating the geometric factor taking into account the retardation were proposed in [86]:

$$F_{g,s} = 2a_s\left[2a_1a_2\left(\frac{1}{D_1}+\frac{1}{D_2}\right)+\ln\frac{D_1}{D_2}\right]+ \\ +\frac{2b_s}{R}\left[8a_1a_2+\left(D_1+D_2\right)\ln\frac{D_1}{D_2}\right],\quad L\le L_s; \tag{71}$$

$$F_{g,L} = \frac{2a_L}{5R}\left[4a_1a_2\left(\frac{z_+^2}{D_1^2}+\frac{z_-^2}{D_2^2}\right)-\frac{2\left(z_+^2-a_1a_2\right)}{D_1}+ \right. \\ +\frac{2\left(z_-^2+a_1a_2\right)}{D_2}+\ln\frac{D_2}{D_1}\left.\right]+\frac{2b_L}{15}\left[\frac{1}{D_2}-\frac{1}{D_1}+ \right. \\ +\frac{2\left(z_+^2-a_1a_2\right)}{D_1^2}-\frac{2\left(z_-^2+a_1a_2\right)}{D_2^2}- \\ \left.-8a_1a_2\left(\frac{z_+^2}{D_1^3}+\frac{z_-^2}{D_2^3}\right)\right],\quad L>L_s; \tag{72}$$

where $a_s = 1.01$, $b_s = 0.28\pi/\lambda_0$, $a_L = 2.45\lambda_0/2\pi$, $b_L = 2.04(\lambda_0/2\pi)^2$, $z_\pm = a_1 \pm a_2$, the values of D_1 and D_2 are defined by the expressions

$$D_1 = R^2 - z_+^2,\quad D_2 = R^2 - z_-^2. \tag{73}$$

The interparticle transition distance from formula (71) to (72) in [86] was proposed to be determined by the formula

$$L_s = 109 - 107\lg\left(\sqrt{a_1a_2}\right)+ \\ +37.5\left[\lg\left(\sqrt{a_1a_2}\right)\right]^2 - 4.5\left[\lg\left(\sqrt{a_1a_2}\right)\right]^3 \tag{74}$$

where a_1, a_2 and L_s are expressed in nanometers. Note that due to the dependence of the value of L_s on the radii of nanoparticles, a small jump of the geometric factor may occur when passing from (71) to (72) (see below).

In [87] the approximation (70) was also used and five different formulas for the geometric factor for five distance intervals in the general case of particles of different radii were obtained. The analysis has shown that for the extreme intervals on the small and large distance sides the obtained formulas coincide with the formulas from [86], but the formulas for the inner intervals contain errors, which has already been mentioned in [54].

In [88] the approximation was used as follows

$$f\left(p\right) = \frac{c}{p+c},\quad c = \frac{3.1\lambda_0}{2\pi}, \tag{75}$$

and a sufficiently long expression for the geometric factor was obtained taking into account the lag effects.

In [89] the approximation was used as follows

$$f\left(p\right) = \frac{L_b}{\sqrt{r^2+L_b^2}},\quad L_b = \frac{23}{3\pi}\frac{\lambda_0}{2\pi}, \tag{76}$$

and an expression for the geometrical factor taking into account the retardation effects for particles of equal size was obtained. The expression obtained in [89] can be easily generalized to a more accurate approximation of the retardation factor proposed in the same work:

$$f\left(p\right) = \frac{\xi_1 L_{b,1}}{\sqrt{r^2+L_{b,1}^2}}+\frac{\xi_2 L_{b,2}}{\sqrt{r^2+L_{b,2}^2}}, \\ \xi_1 = 0.462,\ L_{b,1} = 0.485L_b, \\ \xi_2 = 0.538,\ L_{b,2} = 1.443L_b. \tag{77}$$

(For a number of other forms of approximation of the lagging factor, see [90]). The formula for calculating the geometric factor obtained in this paper within the framework of the model proposed in [89] is given in Appendix B.

In Fig. 3 we compare the values of the geometric factor taking into account the retardation from [86, 88] and calculated from expression (86) with the retardation factor (77) proposed in [89]. The following conclusions can be drawn from the analysis of the presented data.

1. For small values of particle radii (up to about 100 nm), all three data sets result in nearly coincident values of the geometric factor up to $L < 10^3 - 10^4$ nm, with a relative error of less than 15%.

2. For particles with a radius of about 1 μm, one can see a marked difference between the calculations according to [86] in the vicinity of the transition point L_s from one formula (71) to another (72). From the comparison of curves 6 and 7 it can be seen that it is impossible to provide a smooth transition from one formula to another. In this case, the data according to [88] and those obtained from (86) again practically coincide and the relative error again does not exceed 15%.

3. After the transition region, all three works lead to geometric factor values differing by no more than 15%.

4. At large values of $L > 10^3 - 10^4$ nm, the calculations of the geometrical factor according to [88] and from expression (86) lose their accuracy and are unacceptable for the calculations. The same happens

at calculations according to formulas from [86], but at values of the interparticle distance greater by an order of magnitude. The loss of accuracy of calculations is caused by the fact that the geometrical factor is calculated as a difference of several values exceeding the desired value by many orders of magnitude. This can (and does, as can be seen from Fig. 3) lead to the wrong sign of the geometric factor even when calculating with numbers with double precision. For example, expression (72) contains terms decreasing as R^{-3}, and the geometric factor at large distances decreases as R^{-7} (see below).

Note that the approach used in [86-89], which summarizes the interaction of each atom of one particle with each atom of another particle, does not allow us to obtain accurate values of the geometric factor with the retardation, and the error can reach 15%, as can be seen from the comparison of the retardation factors for the mutual atom-atom and atom-plane actions in [77] (see also [85]).

When calculating the geometric factor according to formula (72) when the condition $(a_1^2 + a_2^2) / R^2 \ll 1$ is fulfilled, the difficulties noted above arise, so let us present this formula as a sum of series:

$$F_{g,L} = \frac{64a_1^3a_2^3}{5R^7}\times$$
$$\times\sum_{n=0}\frac{(n+2)(n+3)(2n+5)}{R^{2n}}\left(\frac{a_L}{n+3}-\frac{b_L}{3R}\right)\times \quad (78)$$
$$\times\sum_{k=0}^{n}\frac{(k+1)(n-k+1)(2n+3)!}{(2k+3)!(2n-2k+3)!}a_1^{2k}a_2^{2n-2k}.$$

From (78) we see – at large distances the van der Waals interaction potential decreases as R^{-7}. Note that if the condition $(a_1^2 + a_2^2)/R^2 \le 10^{-3}$ is fulfilled, the first two terms of series (78) with $n = 0$ and 1:

$$F_{g,L} \approx \frac{64a_1^3a_2^3}{3R^7}\left[\begin{array}{c}\left(a_L-\frac{b_L}{R}\right)+\\ +\frac{7}{5}\left(3a_L-\frac{4b_L}{R}\right)\left(\frac{a_1^2}{R^2}+\frac{a_2^2}{R^2}\right)\end{array}\right], \quad (79)$$

provide relative accuracy of calculations at the level of 10^{-6}.

Fig. 4 shows the dependence of the ratio of the series term (78) with number n to the zero term $n = 0$. It can be seen that with the growth of the interparticle distance, the members of the series with high number n decrease rapidly.

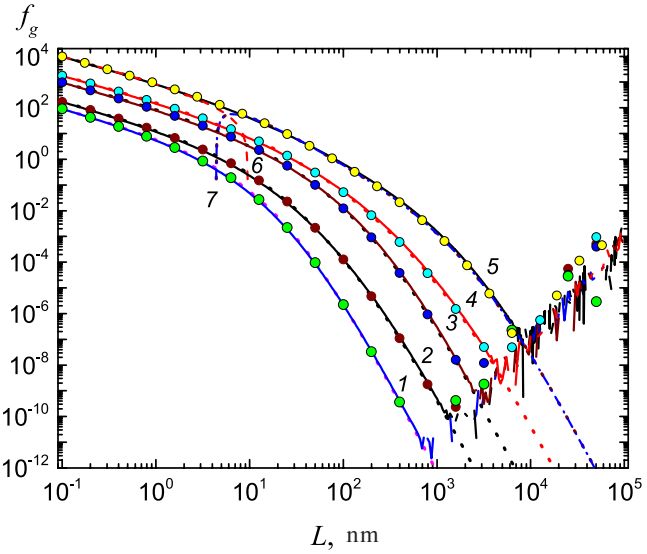

Fig. 3. Dependences of the geometric factor f_g on L according to [88] (solid lines), [86] (dotted lines) and calculated from (86) (black circles) at different particle sizes: curve 1 – $a_1 = a_2 = 10$ nm, 2 – $a_1 = 10$ nm, $a_2 = 100$ nm, 3 – $a_1 = a_2 = 100$ nm, 4 – $a_1 = 100$ nm, $a_2 = 1$ μm, 5 – $a_1 = a_2 = 1$ μm. Curve 6 – expression (71), 7 – (72).

In light of this, the following procedure for calculating the geometric factor with consideration of the retardation is adopted in this paper.

1. At $L \le L_1 = 3\lambda_0/2\pi$, the geometric factor taking into account the retardation was calculated according to [88].

2. At $L > L_1$ (in this case for any pair of atoms the parameter $p > 3$ and the second formula (70) is valid), the geometric factor, taking into account the retardation, was calculated from expression (72) with new values of the parameters a_L and b_L, determined from the continuity condition of the geometric factor and its derivative at the cross-linking point $L = L_1$.

3. When $L > L_2$, where

$$L_2 = \frac{\sqrt{a_1^2 + a_2^2}}{\delta} - (a_1 + a_2),$$

geometric factor was calculated by formula (79). At $L > L_2$ the ratio $(a_1^2 + a_2^2)/R^2$ becomes smaller than δ and the discarded term in the series (78) will be of the order δ^2. In the present work, $\delta = 10^{-5}$ was set to ensure good accuracy and at determining the strength of the interaction.

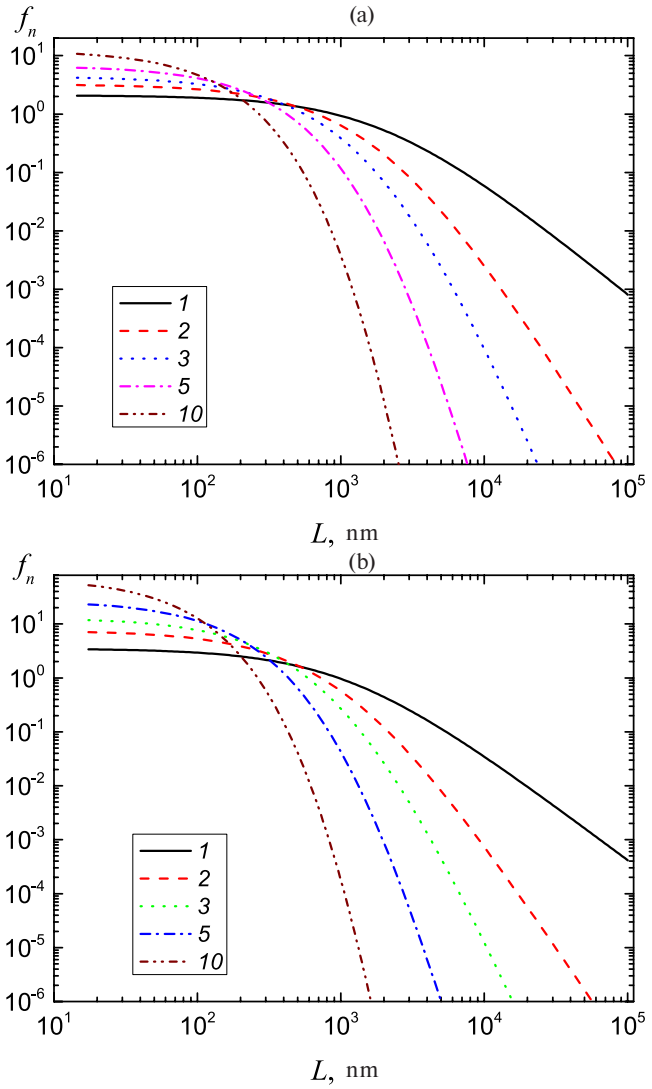

Fig. 4. Ratio of the summand with number n to the summand with number $n = 0$ in the sum (78) for $a_1 = a_2 = 1$ μm (*a*) and $a_1 = 100$ nm, $a_2 = 1$ μm (*b*). The curve numbers correspond to the value of n.

4. NUMERICAL RESULTS AND DISCUSSION

In the present work it was assumed that $\omega_1 \approx \omega_{UV1}$, $\omega_2 \approx \omega_{UV2}$, where ω_{UV1} and ω_{UV2} are the boundaries of absorption zones in the ultraviolet region of the nanoparticle material and the liquid (plasma-forming gas) in which the nanoparticles are located. Argon, which is widely used in dusty plasma studies [10-22], is considered as the plasma-forming gas in this work. For argon, $\varepsilon_2(0) \approx 1$, $\omega_{UV2} = 1.767 \cdot 10^{16}$ c^{-1}, $n_{02}^2 = 1.000282$, $\lambda_0 = 106.66$ nm [91]. The present work will mainly consider spherical particles made of polystyrene, for which the necessary data are well known: at 20°C $\varepsilon_1(0) = 2.557$, $\omega_{UV1} = 1.432 \cdot 10^{16}$ c^{-1}, $n_{01}^2 = 1.447$ [54]. For dust plasma and electrolyte experiments also one uses spherical particles made of polymethyl methacrylate (PMMA), for which at 25°C $\varepsilon_1(0) = 3.6$, $\omega_{UV1} = 6.3 \cdot 10^{15}$ c^{-1}, $n_{01}^2 = 1.492$ and spherical particles made of quartz with properties: $\varepsilon_1(0) = 3.81$, $n_{01}^2 = 2.098$, $\omega_{UV1} = 2.033 \cdot 10^{16}$ c^{-1}.

The system of equations (19) in the case of constant charges or (26) in the case of constant particle surface potentials was solved numerically by the LU decomposition method [75]. The $n_{\max,1}$ terms of the expansion of the potential of the 1st particle and $n_{\max,2}$ terms for the 2nd particle were taken into account, which ensured that the given accuracy was achieved. The necessary number of expansion terms in the case of constant charges was determined from the condition (see expressions (22) and (23)):

$$(2n+1)\frac{K_n(\tilde{R})}{k_1(\tilde{a}_{3-i})} M_n\left(\tilde{a}_i, \varepsilon, \varepsilon_i\right) \le \delta$$

$$for\ n \ge n_{\max,i}, \quad i = 1,2, \tag{80}$$

and in the case of constant potentials from the conditions (see expression (27))

$$(2n+1)\frac{i_n\left(\tilde{a}_i\right)k_n\left(\tilde{R}\right)}{k_n\left(\tilde{a}_i\right)k_0\left(\tilde{a}_{3-i}\right)} \le \delta \text{ for } n \ge n_{\max,i},$$

$$i = 1,2. \tag{81}$$

In this paper, it is assumed that $\delta = 10^{-181}$. The procedure for computing Bessel functions is described in Appendix C.

In Fig. 5 compares the dependences of the total interaction energy $U_t = U_{12} + U_{vdW}$ on the distance between their surfaces at different values of electron and ion concentrations. It can be seen that the potential barrier is very high and its height decreases with increasing concentration. At small distances between particles the attraction due to van der Waals interaction prevails, while the electrostatic interaction between identical particles with equal charges turns out to be repulsive at all distances between particles. In dust plasma, the particle charge appears to be approximately at the level of 10^3 electron charges per micron of particle radius [10, 11, 92, 93], so the potential barrier under these conditions will inhibit the coagulation of particles of the same size.

Fig. 6 shows the dependences of the total interaction energy of identical particles at different values of their charge. It is well seen that the height of the potential barrier practically disappears as the charge

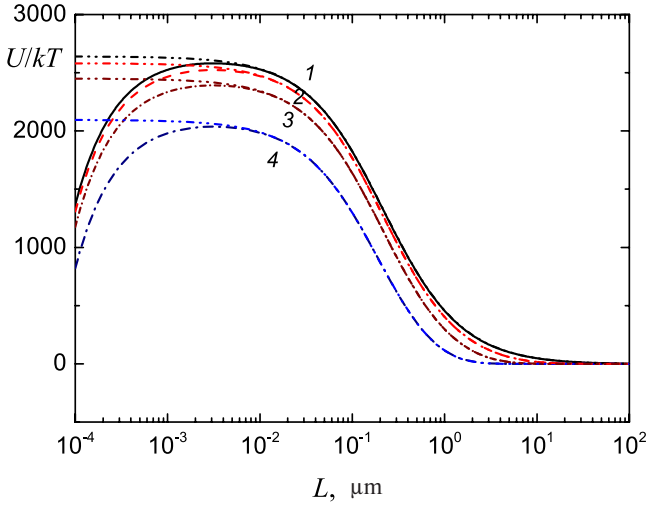

Fig. 5. Total interaction energy of polystyrene particles with radius $a_1 = a_2 = 100$ nm, charges $q_1 = q_2 = 100e$ in argon plasma with different density of charged particles: curve $1 - n_e = n_i = 10^8$ cm^{-3}, $2 - 10^{10}$ cm^{-3}, $3 - 10^{11}$ cm^{-3} , $4 - 10^{12}$ cm^{-3}.

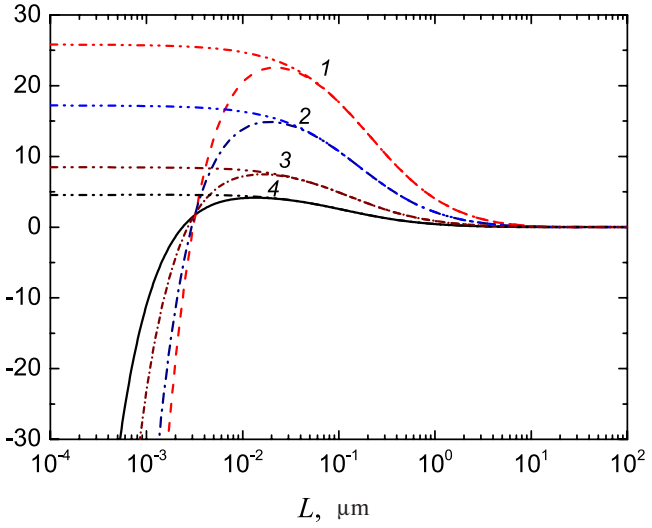

Fig. 7. Total interaction energy of polystyrene particles in argon plasma at $n_e = n_i = 10^{10}$ cm^{-3}, $a_2 = 100$ nm, $q_2 = 10e$ at different values of radius and charge of the 1st particle: curve *1* – $a_1 = 100$ nm, $q_1 = 10e$, *2* – $a_1 = 50$ nm, $q_1 = 5e$, *3* – $a_1 = 20$ nm, $q_1 = 2e$, *4* – $a_1 = 10$ nm, $q_1 = 1e$.

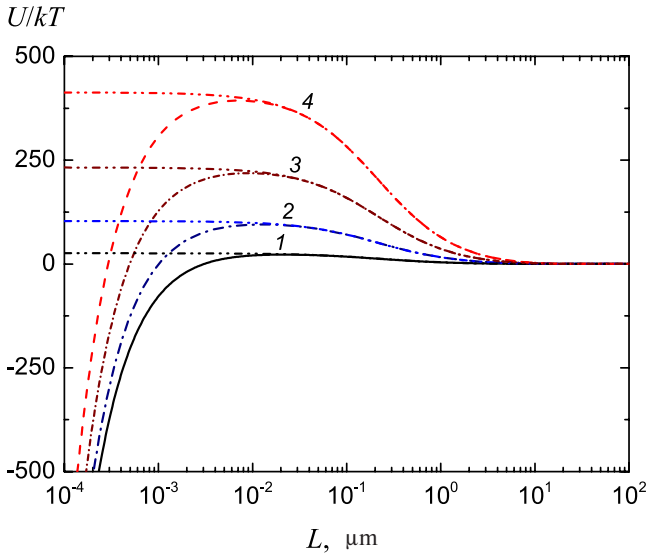

Fig. 6. Total interaction energy of polystyrene particles in argon plasma at $n_e = n_i = 10^{10}$ cm^{-3}, $a_1 = a_2 = 100$ nm at different values of charge: curve *1* – $q_1 = q_2 = 10e$, *2* – $q_1 = q_2 = 20e$, *3* – $q_1 = q_2 = 30e$, *4* – $q_1 = q_2 = 40e$.

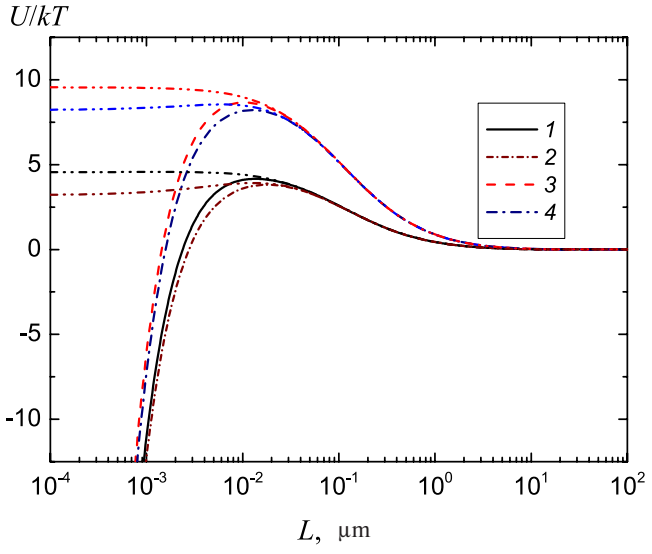

Fig. 8. Total interaction energy of polystyrene particles in argon plasma at $n_e = n_i = 10^{10}$ cm^{-3}, $a_1 = 10$ nm, $a_2 = 100$ nm, with deviation from the linear dependence of particle charge on their radius: curve *1* – $q_1 = 1e$ nm, $q_2 = 10e$, *2* – $q_1 = 2e$ nm, $q_2 = 5e$, *3* – $q_1 = 1e$ nm, $q_2 = 20e$, *4* – $q_1 = 2e$ nm, $q_2 = 10e$

of the particles decreases. As can be seen from Fig. 7, a decrease in the radius of one of the particles (when the charge is proportional to the radius) also leads to a noticeable decrease in the height of the potential barrier.

Fig. 8 investigates the effect of the deviation of the charge of particles from the linear dependence on their radius. It can be seen that at the same value of the product q_1q_2 the violation of the linear dependence leads to the appearance of electrostatic attraction between the particles, while the total interaction turns out to be weakly sensitive to it.

In Fig. 5-8, the dependences of U_{12} on L are indicated by dashed-dotted lines.

5. CONCLUSIONS

The study of the screened electrostatic interaction and van der Waals interaction of dielectric particles has shown that at particle charges characteristic for dusty plasmas of the order of 10^3 electron charges per micron of particle radius the total interaction potential has a sufficiently high barrier, which strongly prevents convergence and coagulation of particles of comparable sizes in the dust plasma. The decrease of radius of one of particles in a pair leads to a noticeable decrease of height of the potential barrier. Also, violation of the linear dependence of the charge on the radius of particles leads to some decrease in the height of the potential barrier, which should be taken into account when modeling the processes of particle coagulation in dusty plasmas. These processes can be important at weak rates of gas ionization by an external ionization source (e.g., products of radioactive decay) and in the Earth's atmosphere, where the attachment of electrons to oxygen molecules leads to a significant decrease in their concentration and a significant decrease in the charge of particles.

FUNDING

This work was financially supported by the RSF (project No. 22-22-01000).

Appendix A.
Computation of coefficients G_{nm}^{ℓ}

The coefficients of G_{nm}^{ℓ} can be easily calculated using recurrence relations:

$$G_{00}^0 = G_{n0}^0 = G_{0m}^0 = 1, \quad n = 1,\infty,\ m = 1,\infty; \quad (82)$$

$$G_{(n+1)m}^0 = G_{nm}^0 \frac{\left(n+1/2\right)(n+m+1)}{(n+1)\left(n+m+1/2\right)},$$

$$n = 0,\ldots,\infty, m = n+1,\infty; \quad (83)$$

$$G_{nm}^{\ell+1} = \frac{(n-\ell)}{\left(n-\ell-1/2\right)}\frac{\left(m-\ell\right)}{\left(m-\ell-1/2\right)}\frac{\left(\ell+1/2\right)}{\left(\ell+1\right)}\times$$
$$\times\frac{\left(n+m-\ell+1/2\right)}{(n+m-\ell)}\frac{\left(n+m-2\ell-3/2\right)}{\left(n+m-2\ell+1/2\right)}G_{nm}^{\ell},$$
$$\ell = 1,\ldots,\infty, n,m > \ell. \quad (84)$$

The calculation of the values of $G_{(n+1)m}^0$ from the relation (83) is first carried out for $n = 0$ and $m = 1,2,\ldots$ consecutively, then for $n = 1$ and $m = 2,3,\ldots$ etc., and the calculation of $G_{\ell}^{\ell+1}$ from the relation (84) is carried out sequentially for $\ell = 0,1,\ldots$ for all necessary values of n and m.

Appendix B.
Geometrical factor with retardation factor $L_b/\sqrt{L_b^2 + r^2}$

Let us introduce the following notations and functions (we do not specify the arguments of functions a_1 and a_2):

$$x_1 = R - a_1 - a_2,\ x_2 = R + a_1 - a_2,$$

$$x_3 = R - a_1 + a_2,\ x_4 = R + a_1 + a_2;$$

$$\gamma_i = \sqrt{L_b^2 + x_i^2}, \zeta_i = L_b + \gamma_i, \tau_i = x_i + \gamma_i,$$

$$i = 1,\ldots,4;$$

$$f_{a,1}\left(R\right) = 2a_1^2\left(a_1 - R\right)+,$$
$$+2a_2^2\left(a_2 - R\right) + R\left(R^2 - a_1^2 - a_2^2\right),$$

$$f_{a,2}\left(R\right) = 4a_1^2 + 4a_2^2 - 3R\left(a_1 + a_2\right) - R^2 - 12a_1a_2,$$

$$f_{b,1}\left(R\right) = 6a_1\left(3a_1 - 5a_2\right) + 5x_2\left(3a_1 - 3a_2 + R\right),$$

$$f_{b,2}\left(R\right) = 9\left(a_1^2 - 5a_2^2 + 5R^2\right) - 160x_2R,$$

$$f_{c,1}\left(R\right) = 48x_1x_4 + 29x_1R + 60a_1a_2,$$

$$f_{c,2}\left(R\right) = 133x_1R - 204x_2x_3 + 36a_1a_2,$$

$$f_1\left(R\right) = 12a_1^2\left(23a_1 - 66a_2\right) +$$
$$+12a_2^2\left(54a_1 - 17a_2\right) +$$
$$+ R\left(17a_1^2 + 337a_2^2 - 426a_1a_2\right) -$$
$$-R^2\left(62a_2 + 71R + 222a_1\right),$$

$$f_2\left(R\right) = a_1^4\left(312a_1 - 660a_2 + 275R\right) -$$
$$- 30a_1^2(a_2 - R)^2(10a_2 + 9R) +$$
$$+ 20a_1(a_2 - R)^3(9a_2 + 13R) -$$
$$-(a_2 - R)^4(48a_2 + 77R) +$$
$$+ 20a_1^3\left(21a_2^2 - 22a_2R + R^2\right).$$

After summarizing (integrating) the interaction of each atom of one particle with each atom of another particle for the geometric factor with the lag factor in the form (76), we obtain

$$\begin{aligned} f_g\left(R,L_b\right) &= \frac{2L_b}{5R}\ln\frac{\tau_2\tau_3}{\tau_1\tau_4} + 2\ln\frac{x_1\zeta_2}{x_2\zeta_1} + 2\ln\frac{x_4\zeta_3}{x_3\zeta_4} + \\ &+ \frac{2a_1^3}{15L_bR}\left\{\frac{\gamma_2}{x_2^4}\left[-2f_{b,1}\left(R\right) + \frac{x_2^2}{L_b^2}f_{b,2}\left(R\right)\right] + \right. \\ &\left. + \frac{\gamma_3}{x_3^4}\left[2f_{b,1}\left(-R\right) - \frac{x_3^2}{L_b^2}f_{b,2}\left(-R\right)\right]\right\} - \\ &- \frac{8a_1^3}{L_b^2R}\left(1 - \frac{3a_1^2}{20L_b^2} - \frac{3R^2 - 3a_2^2}{4L_b^2}\right)\ln\frac{x_2\zeta_3}{x_3\zeta_2} - \\ &- \frac{2}{L_b^2R}\left[f_{a,1}\left(R\right) + \frac{3x_1^3}{40L_b^2}f_{a,2}\left(R\right)\right]\ln\frac{x_1\zeta_2}{x_2\zeta_1} + \\ &+ \frac{2}{L_b^2R}\left[f_{a,1}\left(-R\right) - \frac{3x_4^3}{40L_b^2}f_{a,2}\left(-R\right)\right]\ln\frac{x_4\zeta_3}{x_3\zeta_4} + \\ &+ \frac{1}{30L_bR}\left\{\frac{\gamma_1}{x_1}\left[f_{c,1}\left(R\right) + \frac{x_1^2}{2L_b^2}f_{c,2}\left(R\right)\right] + \right. \\ &\left. + \frac{\gamma_4}{x_4}\left[f_{c,1}\left(-R\right) + \frac{x_4^2}{2L_b^2}f_{c,2}\left(-R\right)\right]\right\} - \\ &- \frac{1}{60L_b^3R}\left[\frac{x_1^2}{x_2^2}\gamma_2 f_1\left(R\right) - \frac{x_4^2}{x_3^2}\gamma_3 f_1\left(-R\right)\right] + \\ &+ \frac{1}{30L_bR}\left[\frac{\gamma_2}{x_2^4}f_2\left(R\right) - \frac{\gamma_3}{x_3^4}f_2\left(-R\right)\right]. \end{aligned} \tag{85}$$

As noted above, in [89] there was given expression for the geometrical factor taking into account the lag effects for particles of equal size (note that in expression (22) for g_{aux} in this work the minus sign before the fourth term in the first row is lost). Calculations have shown that at equal radii expression (85) gives the values of geometrical factor, coinciding with the data of calculations according to the formulas from [89].

With the retardation factor in the form (77) the geometric factor will be defined by the expression

$$f_g\left(R,L_b\right) = \xi_1 f_g\left(R,L_{b,1}\right) + \xi_2 f_g\left(R,L_{b,2}\right). \tag{86}$$

Appendix C. Computation of the modified spherical Bessel functions

Modified spherical Bessel functions at $x = k_D a_i$, $i = 1,2$, were computed using recurrence relations [67]

$$\begin{aligned} k_{n+1}\left(x\right) &= k_{n-1}\left(x\right) + \frac{2n+1}{x}k_n\left(x\right), \\ i_{n-1}\left(x\right) &= i_{n+1}\left(x\right) + \frac{2n+1}{x}i_n\left(x\right). \end{aligned} \tag{87}$$

In the first step, using the first formula (87), the values of $k_n(x)$ for $n = 1,2,\ldots,n_{\max}+1$ ($n_{\max} = 1000$), starting from $k_0(x)$ and $k_1(x)$ were calculated decreasing as n increases:

$$\begin{aligned} k_0(x) &= \frac{\pi}{2x}e^{-x}, \\ k_1(x) &= k_0(x)\left(1 + \frac{1}{x}\right). \end{aligned} \tag{88}$$

In the second step, the ratio i_{n+1}/i_n for $n = n_{\max}$ was calculated based on Gaussian continuous fraction [94]:

$$\frac{i_n\left(x\right)}{i_{n-1}\left(x\right)} = \frac{x}{2n+1}\frac{1}{1 + \dfrac{a_1\left(x\right)}{1 + \dfrac{a_2\left(x\right)}{1+\ldots}}}, \tag{89}$$

where the coefficients a_k are defined by the relations:

$$a_k\left(x\right) = \frac{x^2}{\left(2n+2k-1\right)\left(2n+2k+1\right)}, k = 1,2,\ldots \tag{90}$$

The calculations started with $k = 20$, which ensured high accuracy of the calculation of this ratio. Then, using the relation (24) and already calculated values of $k_n(x)$ for $n = n_{\max}$ and $n_{\max}+1$, we calculate $i_n(x)$ for $n = n_{\max}$ and $n_{\max}+1$. Finally, the values of $i_n(x)$ functions decreasing as n decreases were computed for $n = n_{\max}-1,\ldots,1$ from the second recurrence relation (87). In order to control the accuracy of the calculations, at the last step, the calculated values i_n for $n = 0,1$ were compared with those calculated from known relations:

$$\begin{aligned} i_0(x) &= \frac{\sinh x}{x}, \\ i_1(x) &= -\frac{\sinh^2 x}{x^2} + \frac{\cosh x}{x}. \end{aligned} \tag{91}$$

The modified spherical Bessel functions at $x = k_D R$ were computed based on the first recurrence relation (87) for $n = 0,1,\ldots,n_{\max,2}$.

Here we also give expressions for the derivatives of the modified spherical Bessel functions:

$$\frac{\partial i_n(z)}{\partial z} = i_{n+1}(z) + \frac{n}{z} i_n(z), \qquad \frac{\partial k_n(x)}{\partial x} = -k_{n+1}(x) + \frac{n}{x} k_n(x). \tag{92}$$

REFERENCES

1. J.N. Israelachvili, *Intermolecular and surface forces*; *3rd ed.* (Elsevier, Amsterdam, 2011) pp.191-499.
2. B. Honig, A. Nicholls, *Science* **268**, 1144-1149 (1995).
3. I. Ledezma-Yanez, W. D.Z. Wallace, P. Sebastián-Pascual, V. Climent, J. M. Feliu, M. T. Koper, *Nat. Energy* **2** (4), 17031 (2017).
4. B. Smit, J. A. Reimer, C. M. Oldenburg, I. C. Bourg, Introduction to carbon capture and sequestration, v.1. (*World Scientific*, Singapore, 2014).
5. M. Manciu, E. Ruckenstein, *Langmuir* **17**, 7061-7070 (2001).
6. H. Wennerstrom, E. Vallina Estrada, J. Danielsson, M. Oliveberg, *Proc. Natl. Acad. Sci. USA* **117**, 10113-10121 (2020).
7. S. Su, I. Siretanu, D. van den Ende, B. Mei, G. Mul, F. Mugele, *Adv. Mater.* **33**, 2106229 (2021).
8. D.F. Parsons, M. Boström, P. L. Nostro, B. W. Ninham, *Phys. Chem. Chem. Phys.* **13** (27), 12352-12367 (2011).
9. K. Voïtchovsky, J. J. Kuna, S. A. Contera, E. Tosatti, F. Stellacci, *Nat. Nanotechnol.* **5** (6), 401-405 (2010).
10. V.N. Tsytovich, *Phys. Usp.* **40**, 53-94 (1997).
11. A.P. Nefedov, O. F. Petrov, V. E. Fortov, *Phys. Usp.* **40**, 1163-1173 (1997).
12. V.I. Molotkov, O. F. Petrov, M. Yu. Pustyl'nik, V.M. Torchinskii, V. E. Fortov, A. G. Khrapak, *High Temp.* **42**, 827-841 (2004).
13. S.V. Vladimirov, K. Ostrikov, A. A. Samarian, *Physics and Applications of Complex Plasmas* (London, Imperial College Press, 2005).
14. V.E. Fortov, A. V. Ivlev, S. A. Khrapak, A. G. Khrapak, G. E. Morfill, *Phys. Rep.* **421**, 1 (2005).
15. G.E. Morfill, A. V. Ivlev, *Rev. Mod. Phys.* **81**, 1353 (2009).
16. M. Bonitz, C. Henning, D. Block, *Rep. Prog. Phys.* **73**, 066501 (2010).
17. *Complex and dusty plasma*: *from the laboratory to space*, eds. V. Fortov, G. Morfill. (Science, Fizmatlit, Moscow, 2012) (in Russian).
18. A. Ivlev, H. Lowen, G. Morfill, C. P. Royall, Complex plasmas and colloidal dispersions: particle-resolved studies of classical liquids and solids. *Series in Soft Condensed Matter*, vol. 5 (World Scientific, Singapore, 2012).
19. I. Mann, N. Meyer-Vernet, A. Czechowski, *Phys. Rep.* **536**, 1 (2014).
20. P. K. Shukla and A. A. Mamun, *Introduction to dusty plasma physics* (CRC Press, Bristol and Philadelphia, 2015).
21. A.V. Ivlev, S. A. Khrapak, V. I. Molotkov, A. G. Khrapak, *Introduction to the Physics of Dust and Complex Plasma* (Intellect Publishing House, Moscow, 2017).
22. A.M. Lipaev, V. I. Molotkov, D. I. Zhukhovitskii, V. N. Naumkin, A. D. Usachev, A. V. Zobnin, O. F. Petrov, V. E. Fortov, *High Temp.* **58** (4), 449-475 (2020).
23. I.M. Kennedy, S. J. Harris, *J. Colloid. Interface. Sci.* **130**, 489-497 (1989).
24. P. Patra, A. Roy, *Phys. Rev. Fluids* **7**, 064308, 20 p. (2022).
25. T.B. Jones, T. B. Jones, *Electromechanics of Particles* (Cambridge University Press, Cambridge, 2005).
26. A. Castellanos, *Adv. Phys.* **54** (4), 263-376 (2005).
27. J. Feng, G. Biskos, A. Schmidt-Ott, *Scientific reports* **5**, 1-9 (2015).
28. F. Greiner, A. Melzer, B. Tadsen, S. Groth, C. Killer, F. Kirchschlager, F. Wieben, I. Pilch, H. Kruger, D. Block, A. Piel, S. Wolf, *Eur. Phys. J. D* **72**, 81 (2018).
29. A.R. Wassel, M. E. El-Naggar, K. Shoueir, J. Environ, *Chem. Eng.* **8** 104175, (2020).
30. X. Meng, J. Zhu, and J. Zhang, *J. Phys. D* **42**, 065201 (2009).
31. V. A. Turek, M. P. Cecchini, J. Paget, A. R. Kucernak, A. A. Kornyshev, J. B. Edel, *ACS Nano* **6**, 7789 (2012).
32. P.-P. Fang, S. Chen, H. Deng, M. D. Scanlon, F. Gumy, H. J. Lee, D. Momotenko, V. Amstutz, F. Cortés-Salazar, C. M. Pereira, Z. Yang, H. H. Girault, *ACS Nano* **7**, 9241 (2013).
33. J. B. Edel, A. A. Kornyshev, M. Urbakh, *ACS Nano* **7**, 9526 (2013).
34. B. Gady, D. Schleef, R. Reifenberger, D. Rimai, and L. P. DeMejo, *Phys. Rev. B* **53**, 8065 (1996).
35. 35] B. Gady, R. Reifenberger, D. S. Rimai, L. P. DeMejo, *Langmuir* **13**, 2533-2537 (1997).
36. Y. Liu, C. Song, G. Lv, N. Chen, H. Zhou, X. Jing, *Appl. Surf. Sci.* **433**, 450-457 (2018).
37. M.C. Stevenson, S. P. Beaudoin, and D.S. Corti, *J. Phys. Chem. C* **124** 3014 (2020).
38. M.C. Stevenson, S. P. Beaudoin, and D.S. Corti, *J. Phys. Chem. C* **125** 20003 (2021).

39. H. Zhou, M. Götzinger, W. Peukert, *Powder Technol.* **135-136**, 82-91 (2003).
40. Y. Gao, E. Tian, and J. Mo, *ACS ES&T Eng.* **1**, **10**, 1449-1459 (2021)
41. N.M. Kovalchuk, D. Johnson, V. Sobolev, N. Hilal, V. Starov, *Adv. Colloid. Interface. Sci.* **272**, 102020 (2019).
42. B.V. Derjaguin, N. V. Churaev, V. M. Muller, *Surface Forces* (Consultants Bureau: New York, 1987).
43. E.J.W. Verwey, J. Th.G. Overbeek, *Theory of the Stability of Lyophobic Colloids* (Elsevier, Amsterdam, 1948).
44. A.B. Glendinning, W. B. Russel, *J. Colloid Interface Sci.* **93**, 95-104 (1983).
45. S.L. Carnie, D. Y.C. Chan, J. Colloid, *Interf. Sci.* **161**, 260-264 (1993).
46. A.V. Filippov, I. N. Derbenev, *J. Exp. Theor. Phys.* **123** (6), 1099-1109 (2016).
47. I.N. Derbenev, A. V. Filippov, A. J. Stace, E. Besley, *J. Chem. Phys.* **145**, 084103 (2016), 9 pp.
48. A.V. Filippov, I. N. Derbenev, A. A. Pautov, M. M. Rodin, *J. Exp. Theor. Phys.* **125** (3), 518-529 (2017).
49. I.N. Derbenev, A. V. Filippov, A. J. Stace, E. Besley, *Soft Matter* **14**, 5480-5487 (2018).
50. S.V. Siryk, A. Bendandi, A. Diaspro, W. Rocchia, *J. Chem. Phys.* **155**, 114114 (2021).
51. S.V. Siryk, W. Rocchia, *J. Phys. Chem. B* **126**, 10400 (2022).
52. Y.-K. Yu, *Phys. Rev. E* **102**, 052404 (2020).
53. O.I. Obolensky, T. P. Doerr, Y.-K. Yu, *Eur. Phys. J. E* **44**, 129 (2021).
54. W.R. Bowen, F. Jenner, *Adv. Colloid Interface Sci.* **56**, 201-243 (1995).
55. J.I. Kilpatrick, S.-H. Loh, S. P. Jarvis, *J. Am. Chem. Soc.* **135**, 2628-2634 (2013).
56. S.R. Van Lin, K. K. Grotz, I. Siretanu, N. Schwierz, F. Mugele, *Langmuir* **35**, 5737-5745 (2019).
57. A. Klaassen, F. Liu, F. Mugele, I. Siretan, *Langmuir* **38**, 914-926 (2022).
58. A.V. Filippov, V. M. Starov, *JETP Lett.* **117** (8), 598-605 (2023).
59. A.V. Filippov, V. Starov, *J. Phys. Chem. B* **127**, 6562-6572 (2023).
60. A.V. Filippov, *J. Exp. Theor. Phys.* **109** (3), 516-529 (2009).
61. A.V. Filippov, *Contr. Plasma Phys.* **49**, 433-447 (2009).
62. V.R. Munirov, A. V. Filippov, *J. Exp. Theor. Phys.* **117**, 809-819 (2013).
63. A.V. Filippov, *JETP Letters* **115** (3), 174-180 (2022).
64. A.V. Filippov, *J. Exp. Theor. Phys.* **134** (5), 590-599 (2022).
65. P. Debye, E. Hükel, *Phys. Zeitschr.* **24**, 185-206 (1923).
66. H.S. Carslaw, J. C. Jaeger, *Conduction of Heat in Solids*, 2nd ed. (Clarendon, Oxford, 1959; Nauka, Moscow, 1964).
67. G.N. Watson, *A treatise on the theory of Bessel functions* (Cambridge University Press, 1922, London).
68. D. Langbein, Theory of Van der Waals Attraction, *Springer Tracts in Modern Physics*; v.72, G. Hohler, Ed. (Springer-Verlag, Berlin Heidelberg New York, 1974).
69. V.V. Batygin, I. N. Toptygin, *Problems in Electrodynamics*, 2nd Edition (Academic Press, London, England, 1978).
70. W.R. Smythe, *Static and dynamic electricity*, 2nd ed. (Hemisphere Pub, New York, Toronto, London 1950).
71. V.R. Munirov, A. V. Filippov, *J. Exp. Theor. Phys.* **115**, 527-534 (2012).
72. E.S. Reiner, C. J. Radke, J. Chem, *Soc. Faraday Trans.* 86, 3901-3912 (1990).
73. M.K. Gilson, M. E. Davis, B. A. Luty, J. A. McCammon, *J. Phys. Chem.* **97**, 3591-3600 (1993).
74. B. Lu, X. Cheng, T. Hou, J. A. McCammon, *J. Chem. Phys.* **123**, 084904 (2005).
75. W.H. Press, W. T. Vetterling, S. A. Teukolsky, B. P. Flannery, *Numerical Recipes Example Book* (*FORTRAN*) (Cambridge University Press, Cambridge, 1992).
76. H. C. Hamaker, *Physica* **4**, 1058-1072 (1937).
77. H.B.G. Casimir, D. Polder, *Phys. Rev.* **73**, 360-372 (1948).
78. E.M. Lifshitz, *J. Exp. Theor. Phys. USSR* **2**, 73-83 (1956).
79. I.E. Dzyaloshinskii, E. M. Lifshitz, L. P. Pitaevskii, *J. Exp. Theor. Phys. USSR* **10**, 161-170 (1960).
80. B.V. Derjaguin, I. I. Abrikosova, E. M. Lifshitz, *Phys. Usp.* **58**, 906-924 (2015).
81. Y.S. Barash, V. L. Ginzburg, *Sov. Phys. Usp.* **27**, 467-491 (1984).
82. N.V. Churaev, *Russ. Chem. Rev.* **73**, 25-36 (2004).
83. D.J. Mitchell, B. W. Ninham, *J. Chem. Phys.* **56**, 1117-1126 (1972).
84. R.G. Horn, J. N. Israelachvili, *J. Chem. Phys.* **75**, 1400-1411 (1981).
85. J.Th.G. Overbeek, in "Colloid Science", H.R. Kruyt, Ed., Vol. 1, p. 266 (Elsevier, Amsterdam, 1952).
86. B. Vincent, *J. Colloid. Interf. Sci.* **42**, 270-285 (1973).
87. P. Görner, J. Pich, *J. Aerosol Sci.* **20**, 735-747 (1989).
88. J. Chen, A. Anandarajah, *J. Colloid. Interf. Sci.* **180**, 519-523 (1996).

89. G.Sh. Boltachev, N. B. Volkov, K. A. Nagayev, *J. Colloid. Interf. Sci.* **355**, 417-422 (2011).

90. S.R. Gomes de Sousa, A. Leonel, A. J.F. Bombard, *Smart Mater. Struct.* **29**, 055039 (2020).

91. A.A. Radzig, B. M. Smirnov, *Handbook of Atomic and Molecular Physics* (Atomizdat, Moscow, 1980) (in Russian).

92. A.V. Filippov, N. A. Dyatko, A. S. Kostenko, *J. Exp. Theor. Phys.* **119** (5), 985-995 (2014).

93. A.V. Filippov, V. N. Babichev, A. F. Pal', A.N. Starostin, V. E. Cherkovets, V. K. Rerikh, M. D. Taran, *Plasma Phys. Rep.* **41** (11), 895-904 (2015).

94. W. Gautschi, J. Slavik, *Math. Comput.* **32**, 865-875 (1978).